RSC Advances

PAPER

View Article Online
View Journal | View Issue

Cite this: *RSC Adv.*, 2023, **13**, 1853

Electron beam irradiation grafting of metal–organic frameworks onto cotton to prepare antimicrobial textiles†

Zepeng Liu,[ab] Ziqiang Wang,[b] Yu Meng,[a] Yongchang Song,[a] Linfan Li,*[b] Ming Yu*[a] and Jingye Li[ab]

Received 10th November 2022
Accepted 23rd December 2022

DOI: 10.1039/d2ra07144d

rsc.li/rsc-advances

Textiles modified with antimicrobial nanomaterials have excellent comprehensive performance. However, the shedding of nanoparticles often occurs in actual use. This not only reduces the service life of antimicrobial textiles, but also causes potential harm. Here, we report a new method to covalently immobilize a zinc-imidazolate MOF (ZIF-8) onto cotton fabric by electron beam irradiation to prepare antimicrobial textiles with excellent durability. A series of characterization analysis showed the electron beam irradiation did not damage the structure of the ZIF-8 nanoparticles and the particles were successfully introduced onto cotton fibers *via* poly hydroxyethyl acrylate (PHEA). The modified cotton fabric exhibited >99% inhibition of *Escherichia coli*, *Staphylococcus aureus* and *Candida albicans*. The results of dry cleaning and rub resistance tests showed that the prepared antimicrobial cotton fabric had significant durability which was attributed to the strong covalent binding between the MOF and textile.

1. Introduction

Certain species of microorganisms can cause infections in humans, which in turn leads to various diseases.[1] Treating such infections with antibiotics is usually used as a conventional strategy.[2] However, abuse of antibiotics has led to the emergence of drug-resistant and multi-drug-resistant bacteria.[3] Extensively using antimicrobial materials will help to mitigate the risk of the infections by killing microbes to reduce their exposure to people.[4] Many substances can be used as effective antimicrobial ingredients in antimicrobial materials, such as nanozymes.[5] Unlike natural enzymes, nanozymes are simple to synthesize,[6] easy to control,[7] stable[8] and have high catalytic activity.[9] One representative nanoenzyme is metal–organic frameworks (MOFs), a crystalline porous material with high specific surface area.[10]

MOFs and their derivatives are of great recent interest for multiple applications, such as adsorption,[11] separation[12] and catalysis.[13] They also have antimicrobial properties[14] by the following mechanisms: (1) metal ions and ligands have antimicrobial activity, and slow release in the environment can make them have long-lasting antimicrobial activity;[15] (2) loading antimicrobial drugs in their pores can make active substances slowly released into the environment;[16] (3) using MOFs with catalytic activity, active substances such as reactive oxygen species (ROS) are produced under certain conditions and released into the environment, thus kill microorganisms.[17] As one kind of MOFs, ZIF-8 has good biocompatibility[18] and is receiving increasing attention for applications in bioimaging,[19] drug controlled-release,[20] photothermal therapy[21] and photodynamic therapy.[22] According to the study of Taheri *et al.*,[23,24] ZIF-8 can release zinc ions slowly into the environment, giving it good antimicrobial activity and superiority over zinc oxide. Also, according to the study of Li *et al.*,[25] the photocatalytic ability possessed by ZIF-8 itself can also be used for antimicrobial purposes, and its ability is better than other kinds of MOFs.

For producing antimicrobial materials, adding antimicrobial nanoparticles to substrates is a common strategy.[26] Although this simple combination can prepare materials with good antimicrobial properties, their antimicrobial active substances will gradually shed during daily use,[27] causing a decline in antimicrobial properties and even potential harm.[28] Thus, there is an urgent need to develop durable antimicrobial composites that firmly bond antimicrobial active substances to the substrates. Radiation grafting has gradually become an effective means to develop new materials with excellent properties or to modify conventional materials.[29] Radiation grafting uses high energy radiation such as cobalt source,[30] electron beam,[31] and plasma[32] to generate free radical active sites on polymer substrates, which in turn trigger the polymerization of monomers at the active sites to generate grafted chains. As one kind of radiation grafting method, co-irradiation grafting method

[a]*MOE Key Laboratory of Resource Chemistry, Shanghai Key Laboratory of Rare Earth Functional Materials, College of Chemistry and Materials Science, Shanghai Normal University, Shanghai 200234, China. E-mail: yuming@shnu.edu.cn*

[b]*Shanghai Institute of Applied Physics, Chinese Academy of Sciences, Shanghai 201800, China. E-mail: lilinfan@sinap.ac.cn*

† Electronic supplementary information (ESI) available. See DOI: https://doi.org/10.1039/d2ra07144d

has many advantages, including ease of operation,[33] high energy efficiency[34] and wide applicability.[35,36] For example, Yu *et al.*[37] prepared a washing-resistant self-cleaning cotton fabric by co-irradiated grafting of surface double bond modified nano-TiO_2 with hydroxyethyl acrylate on the surface of the cotton fabric. They also studied the grafting and covalent fixation of MIL-101 MOFs onto nylon by gamma irradiation, creating a new method to functionalize and dye nylon.[38] In addition, literature reports have demonstrated the good biocompatibility and excellent mechanical properties of PHEA.[39] The use of PHEA to attach ZIF-8 to cotton is a good option.

In this study, MOF particles were attached to fibers of cotton fabric through poly hydroxyethyl acrylate (PHEA) using electron beam radiation grafting. After absorbing the ethanol mixture of ZIF-8 and hydroxyethyl acrylate (HEA), the cotton fabric was irradiated by electron beam. And the electron beam irradiation triggered the grafting reaction of ZIF-8 and the polymerization reaction of HEA onto the cotton fabric. In this process, HEA polymerizes to form PHEA, and ZIF-8 particles are attached to cotton fibers *via* PHEA chains. That is, one end of the PHEA chain is attached to the cotton fiber and the other end is connected to the ZIF-8 particles. The material obtained by the above process was named as cotton-*g*-ZIF-8. Although PHEA acts as the connecting part, the naming emphasizes the combination of ZIF-8 and cotton in this way. Antimicrobial performance test proved that the prepared cotton fabric has better antimicrobial properties. Dry cleaning and rub resistance tests proved the durability of the prepared cotton-*g*-ZIF-8. Thus, this kind of cotton fabric can provide long-lasting antimicrobial ability through the covalent bonding of ZIF-8 to it. The electron accelerator is a safe, reliable and easy to use device.[40,41] And a certain dose of electron beam irradiation has almost no effect on the mechanical properties of cotton fabric.[42,43] Thus, irradiation grafting using electron beam holds promise for the rapid preparation of such antimicrobial cottons in large quantities.

2. Experimental

2.1. Materials

Zinc nitrate hexahydrate, 2-methylimidazole, methanol, ethanol and tetrachloroethene were purchased from Sinopharm Chemical Reagent Co., Ltd. (Shanghai, China). 2-Hydroxyethyl acrylate (HEA) was purchased from Tokyo Chemical Industry Co., Ltd. (Tokyo, Japan). Cotton fabric was purchased from the market. All reagents were used without further purification.

2.2. Synthesis of ZIF-8 and its radiation effect

2.2.1. Synthesis of ZIF-8. ZIF-8 was synthesized according to the method of Cravillon *et al.*[44] at room temperature. $Zn(NO_3)_3 \cdot 6H_2O$ (734.4 mg at 2.469 mmol) and 2-methylimidazole (810.6 mg at 9.874 mmol) were each dissolved in methanol (50 mL). Stirred to dissolve it fully. Then poured the latter solution into the former solution. After stirring well, it was left to stand for 24 hours. After that, the solution was placed in a centrifuge tube and centrifuged. The supernatant was discarded and the precipitate was washed three times with methanol. Finally, the product was dried in a vacuum oven at 120 °C for 12 hours. The product obtained was some white powder.

2.2.2. Radiation effect of ZIF-8. The synthesized ZIF-8 was irradiated using electron beams at an absorbed dose of 50 kGy in air and nitrogen atmosphere, respectively. ZIF-8 was also added to ethanol and 20 wt% HEA ethanol solution (here, excluding the solvent, the actual mass of HEA is 50% of the total mass) separately and irradiated using electron beams at an absorbed dose of 50 kGy. After irradiation, the latter two mixture samples were placed in centrifuge tubes and centrifuged. The supernatant was discarded and the precipitate was washed three times with ethanol. Finally, all the samples were dried in an oven at 60 °C for 12 hours. Here, the reaction product of ZIF-8 and HEA was named as ZIF-8-*g*-PHEA (this indicates the combination of ZIF-8 and PHEA).

2.3. Synthesis of cotton-*g*-ZIF-8

First, ZIF-8 was uniformly dispersed in the HEA ethanol solution by ultrasonic dispersion process. Then the mixture was sprayed evenly on the cotton fabric. After that, the cotton fabric carrying the mixed solution was put into a vacuum bag and vacuum sealed. Here, excluding the solvent, the addition amount of ZIF-8 is 1% of the total mass, and the addition amount of HEA is 5% of the total mass. It was then irradiated by electron beam at an absorbed dose of 50 kGy. After the irradiation, the cotton fabric was thoroughly washed with water. Finally, the cotton fabric was put into a 60 °C blast drying oven and dried to constant weight.

2.4. Characterization

The Fourier transform infrared (FTIR) spectra were recorded in the range 4000–400 cm^{-1} on a TENSOR 27 instrument from BRUKER, Germany. The powder samples were pressed with KBr in a ratio of 1 : 100, and then the curves were analyzed in transmittance mode. The cotton samples were analyzed in attenuated total reflectance method.

The thermogravimetric analysis (TGA) and differential scanning calorimetry (DSC) was carried out using a STA 449 F3 instrument from NETZSCH in the temperature range of 35–800 °C under N_2 flow at a heating rate of 10 °C min^{-1}. The N_2 flow rate was 40 mL min^{-1}.

The X-ray diffraction (XRD) patterns of the samples were measured by a D8 Advance X-ray tester from BRUKER, Germany. Before the test, the powder samples were ground flat on the surface of the sample stage. Measurement conditions: X-ray diffractometer with Cu Kα target (λ = 1.54 Å), tube voltage of 40 kV, current of 40 mA, scanning range of 5°–90° (2θ), scanning speed of 8° min^{-1}.

The X-ray photoelectron spectroscopy (XPS) was performed on an Ultra DLD type instrument from Kratos Axis, UK. The source gun type was Al Kα with 300 μm spot size. The full spectral flux energy was 150 eV. The elemental spectral flux energy was 60 eV.

The scanning electron microscope (SEM) images were obtained on a Merlin compact instrument from Zeiss, Germany. Test conditions: the surface of the sample was deposited with gold spray, and the scanning voltage was 3–15 kV. The energy dispersive spectroscopy (EDS) images were obtained with the SEM tests.

The water contact angle of the samples before and after irradiation was tested by placing the sample on a glass sheet and flattening it. Then tested on a THETA Optical Tensiometer from KSV, Finland. The test droplet is deionized water with a droplet volume of 5 μL at temperature of 25 °C.

The BET specific surface area of the irradiated products was measured on a V-sorb 2800TP specific surface area tester of Gold APP Instrument Corporation China, Beijing. Test conditions: pretreatment temperature was 120 °C and pretreatment time was 2 h.

The ESR characterization was done on an FA 200 electron spin resonance instrument from JEOL, Japan. The sample state was a solid powder. Test conditions: sweep width 50 mT, microwave frequency 9078 MHz, microwave power 1 mW.

2.5. Antimicrobial performance test of cotton-*g*-ZIF-8

The antimicrobial performance test of the samples was processed according to the standard of GB/T 20944.2-2007 Textiles—Evaluation for antibacterial activity—Part 2: absorption method. The tested strains were *Escherichia coli* 8099, *Staphylococcus aureus* ATCC 6538 and *Candida albicans* ATCC 10231. The samples and control samples were treated with 121 °C for 15 minutes. Calculate the inhibition rate according to eqn (1):

$$\text{Inhibition rate} = \frac{C_t - T_t}{C_t} \times 100\% \quad (1)$$

where C_t represents the average of microbial counts measured after inoculation and incubation of three control samples for 24 hours, and T_t represents the average of microbial counts measured after inoculation and incubation of three samples for 24 hours.

2.6. Dry cleaning and rub resistance tests of cotton-*g*-ZIF-8

The dry-cleaning resistance test was conducted with the standard of ISO 105-D01. A small sample of cotton-*g*-ZIF-8 was cut and placed in tetrachloroethylene and agitated at 30 °C for 30 minutes. The sample was then dried in an oven at 60 °C.

The rub resistance test is carried out according to the standard of ISO 105-X12. A small sample of cotton-*g*-ZIF-8 was cut and placed on a rubbing resistance tester for dry rubbing test. The metal post head with a vertical pressure of 9 N was rubbed back and forth along the track 2000 times in a straight line at a rate of one round trip per second.

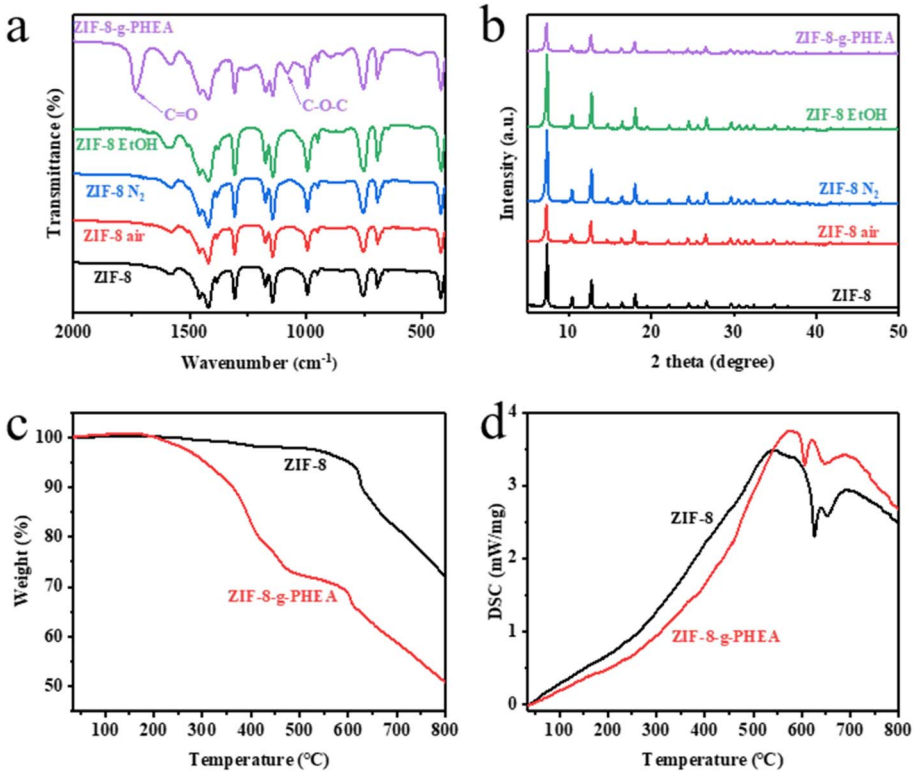

Fig. 1 ZIF-8 and its radiation effect. (a) FTIR spectra of ZIF-8 and its irradiated products (at an absorbed dose of 50 kGy) in different environments. (b) XRD patterns of ZIF-8 and its irradiated products (at an absorbed dose of 50 kGy) in different environments. (c) TGA curves of ZIF-8 and ZIF-8-*g*-PHEA. (d) DSC curves of ZIF-8 and ZIF-8-*g*-PHEA. (d) XRD patterns of ZIF-8 and its irradiated products (at an absorbed dose of 50 kGy) in different environments.

3. Results and discussion

3.1. Radiation effect of ZIF-8

From the FTIR spectrum of ZIF-8 in Fig. 1a, the peak at 1584 cm^{-1} is considered to be the stretching of the C=N bond,[45] while the stretching of the imidazole ring is at 1350–1500 cm^{-1}. The bands in the range of 900–1350 cm^{-1} are the in-plane bending of the imidazole ring, while the peaks below 800 cm^{-1} are the out-of-plane bending. The peak at 421 cm^{-1} is a stretching of the Zn–N bond.[46] It is clear that ZIF-8 was successfully prepared. By comparing the FTIR spectra of the pristine ZIF-8 and the irradiated ZIF-8 in different environments, including air, nitrogen, and ethanol, it can be seen that there is no significant change. It indicates that the ZIF-8 in different environments irradiated by electron beam at a certain absorbed dose has almost no change in chemical composition. But comparing the FTIR spectra of pristine ZIF-8 and ZIF-8-*g*-PHEA, it can be found that the irradiation product of HEA is partially grafted onto ZIF-8, which adds some C=O and C–O–C characteristic groups from PHEA. Fig. 1a shows this change. Under electron beam irradiation, HEA polymerization occurs to produce PHEA. Meanwhile, the free radicals generated by ZIF-8 under electron beam irradiation are combined with PHEA. By this reaction PHEA is attached to the ZIF-8 surface.

The TGA curves of ZIF-8 before and after the irradiation reaction are shown in Fig. 1c. The decomposition of ZIF-8 particles starts at 600 °C. The decomposition of ZIF-8-*g*-PHEA particles can be divided into two processes. The first decomposition started at 200 °C, which is mainly the thermal decomposition of PHEA. The second stage decomposition is similar with ZIF-8 at 600 °C, which is mainly caused by the carbonation of organic components in ZIF-8.[47] The results of TGA curves showed that the HEA irradiation product was successfully introduced onto ZIF-8. On the other hand, the DSC curves also reflect the difference in the thermal decomposition processes of ZIF-8 and ZIF-8-PHEA. This can be visualized in Fig. 1d.

From the XRD patterns in Fig. 1b, we can find that the peaks at 7.35°, 10.40°, 12.75°, 14.74°, 16.49° and 18.07° correspond to the (110), (200), (211), (220), (310), (222) indices of ZIF-8 crystal face, respectively. This is in full agreement with that reported in the ref.[44]. It proves that ZIF-8 crystal was successfully synthesized. The XRD patterns of ZIF-8 after irradiation under different conditions are also presented in Fig. 1b. After irradiation of ZIF-8 particles under air atmosphere, nitrogen atmosphere and ethanol solution at 50 kGy, respectively. It is found that the positions of XRD characteristic peaks do not change, indicating that irradiation does not affect the crystal structure of ZIF-8 in different kind of environments. The characteristic peak of ZIF-8 remained in the XRD pattern of ZIF-8-*g*-PHEA, and no spurious peak appeared. This indicates that the characteristic crystal structure of ZIF-8 still exists after irradiation reaction with HEA, and PHEA was only partially grafted onto the surface of ZIF-8 particles.

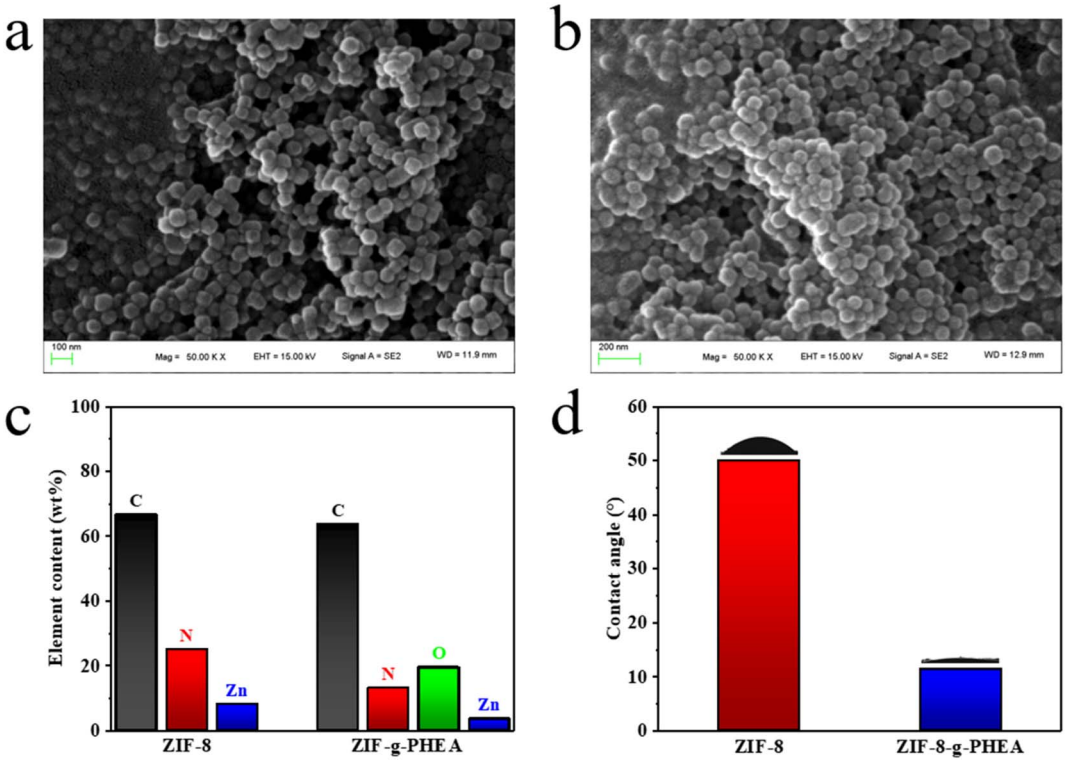

Fig. 2 (a) SEM image of ZIF-8. (b) SEM image of ZIF-8-*g*-PHEA. (c) element analysis of ZIF-8 and ZIF-8-*g*-PHEA (from XPS). (d) water contact angle of ZIF-8 and ZIF-8-*g*-PHEA.

The XPS spectra of ZIF-8 and ZIF-8-*g*-PHEA were analyzed. As can be seen in Fig. S2a,† the characteristic peaks of the major elements such as carbon, nitrogen, oxygen and zinc are still present in the irradiated products. From the C_{1s} spectral splitting curves of ZIF-8 and ZIF-8-*g*-PHEA in Fig. S2b,† it can be found that different binding energies of carbon element exist in the irradiated samples. The three different chemical bonds C–O (286.5 eV), C═O (288.5 eV) and O–C═O (289.2 eV) are from the PHEA component. The results of XPS characterization demonstrated that the irradiation reaction of ZIF-8 with HEA proceeded successfully as expected. The PHEA is attached to the ZIF-8 by a covalent bond.

The BET specific surface areas of ZIF-8 and its irradiated products are obtained from Fig. S6 and S7.† There is a slight decrease in the BET specific surface area of ZIF-8 after irradiation in air and nitrogen atmosphere. This indicates that there is a slight damage to the crystal by the electron beam irradiation at this absorbed dose. In contrast, the BET specific surface area increased after irradiation in ethanol. This may be caused by the migration of the solvent guest molecules in the ZIF-8 pores to ethanol under this effect, which in turn is washed away.[48] And there was a significant decrease in the BET specific surface area of ZIF-8-*g*-PHEA, which could be due to the grafting of PHEA polymer to the surface of ZIF-8, thus partially blocking the pore channels of ZIF-8.

The ESR test results are shown in Fig. S1.† ZIF-8 produced free radicals after irradiation. The measured peak strength was not high, probably due to the decay of free radicals. This can be explained by the study by Li *et al.*[25] However, there were no free radicals in ZIF-8-*g*-PHEA, which indicated that the free radicals produced by irradiation were coupled after co-irradiation polymerization, and the polymer was stable.

SEM images of ZIF-8 and ZIF-8-*g*-PHEA particles at a magnification of 50 000× are shown in Fig. 2a and b, respectively. The average particle size of the synthesized ZIF-8 was 65 nm. According to the figures, it can be found that the morphology of ZIF-8 particles did not change much before and after irradiation. Element analysis in Fig. 2c shows the presence of a significant amount of oxygen element in ZIF-8-*g*-PHEA, which is different from ZIF-8 itself. That demonstrates the grafting of PHEA onto the surface of ZIF-8 particles. In addition, it can be seen in Fig. 2d that the water contact angle of ZIF-8 changed significantly before and after the reaction with HEA, as from 50.0° to 11.4°. This change originates from the combination with PHEA, which adds more hydrophilic hydroxyl groups.

3.2. Characterization of cotton-*g*-ZIF-8

As mentioned previously, cotton-*g*-ZIF-8 was synthesized by covalently immobilizing ZIF-8 onto cotton fibers through PHEA

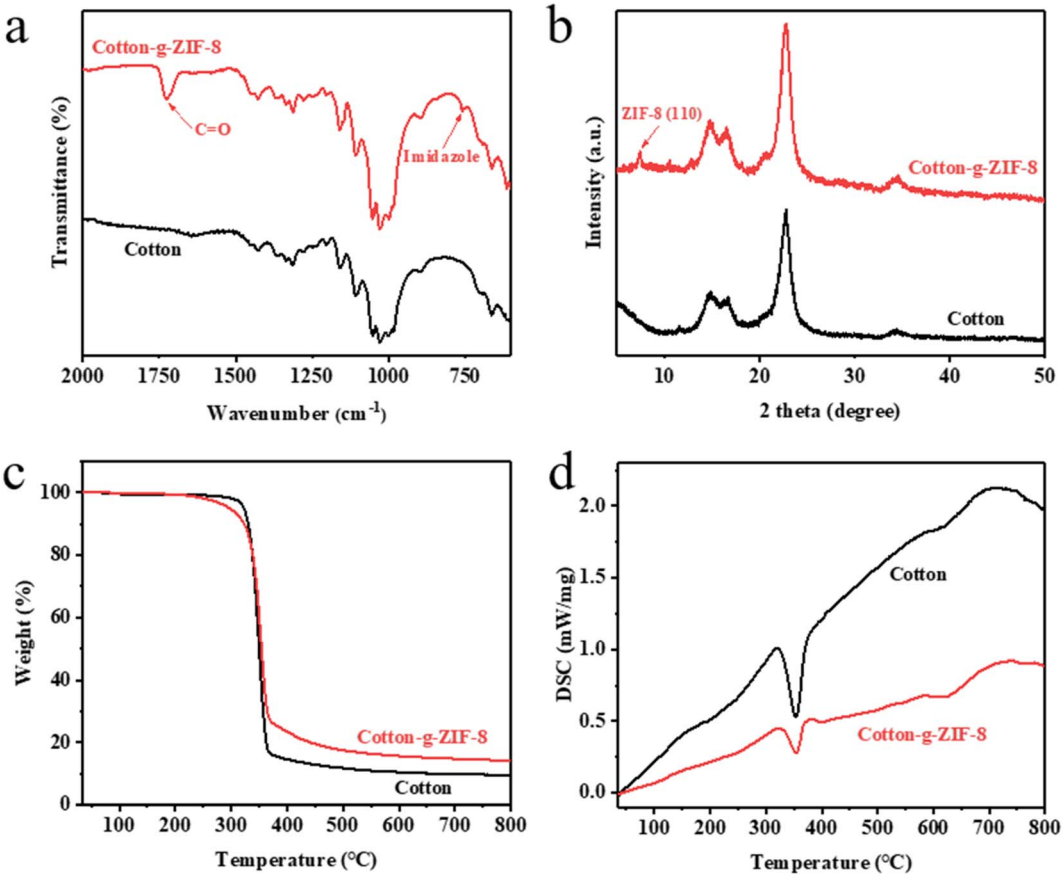

Fig. 3 Characterization of cotton-*g*-ZIF-8. (a) FTIR spectra of cotton and cotton-*g*-ZIF-8. (b) XRD patterns of cotton and cotton-*g*-ZIF-8. (c) TGA curves of cotton and cotton-*g*-ZIF-8. (d) DSC curves of cotton and cotton-*g*-ZIF-8.

chains using a co-radiation grafting method. By comparing the FTIR spectra of pristine cotton and cotton-*g*-ZIF-8, it is known that the ZIF-8 was successfully grafted onto cotton, which adds some C═O and imidazole groups onto it. That can be found the change of peaks in Fig. 3a.

The TGA curves of cotton and cotton-*g*-ZIF-8 are shown in Fig. 3c. The thermal decomposition of pristine cotton occurred rapidly at 350 °C, and there was no significant weight change before 300 °C. The PHEA in cotton-*g*-ZIF-8 started to thermally decompose at 200 °C. From the DSC curves shown in Fig. 3d, it can be found that both cotton and cotton-*g*-ZIF-8 have a significant heat absorption process at 350 °C. The thermal decomposition of cellulose occurs at this temperature. While the DSC curve of cotton-*g*-ZIF-8 shows a heat absorption process at 600 °C. This is most likely the thermal decomposition of ZIF-8.

The XRD patterns of cotton and cotton-*g*-ZIF-8 are presented in Fig. 3b. The XRD pattern of cotton-*g*-ZIF-8 shows a more pronounced diffraction peak at 7.35°, which is the (110) crystallographic plane diffraction peak of ZIF-8. Two diffraction peaks at 10.40° and 12.75° can also be found, which correspond to the (200) and (211) crystallographic diffraction peaks of ZIF-8.

The XPS spectra of cotton and cotton-*g*-ZIF-8 were analyzed. As can be seen in Fig. S3a,† the characteristic peaks of the major elements such as carbon and oxygen are still present in cotton-*g*-ZIF-8. Elemental peaks of nitrogen and zinc specific to ZIF-8 were also present in the XPS spectra of cotton-*g*-ZIF-8. From the C_{1s} spectral splitting curves of cotton and cotton-*g*-ZIF-8 in Fig. S3b,† it can be found that different binding energies of carbon element exist in the irradiated samples. The results of XPS characterization demonstrated that the irradiation reaction of cotton with ZIF-8 and HEA proceeded successfully as expected, with the addition of some covalently bonded ZIF-8-PHEA after the reaction.

SEM images of cotton-*g*-ZIF-8 are shown in Fig. 4a and b. Fig. 4a is an SEM picture of cotton-*g*-ZIF-8 at a magnification of 2000 times with partial zoom. It can be seen that the ZIF-8 particles are more uniformly attached to the surface of the cotton fiber. From EDS analysis pictures Fig. S4,† except carbon and oxygen elements of the original cotton, the cotton-*g*-ZIF-8 fiber surface is also sparsely distributed with nitrogen and zinc elements that are unique to ZIF-8. This indicates that ZIF-8 particles were successfully distributed on the surface of cotton fibers. Element analysis in Fig. 4c shows the presence of a several of nitrogen and zinc element in cotton-*g*-ZIF-8, which is different from cotton itself. That demonstrates the grafting of ZIF-8 onto the surface of cotton fabric. Moreover, Fig. 4d showed that the water contact angle of cotton fabric changed significantly before and after the reaction with ZIF-8, as from 70.4° to 26.7°. This change originates from the combination with ZIF-8 and PHEA, which adds more hydrophilic groups.

3.3. Antimicrobial performance of cotton-*g*-ZIF-8

The data from the antimicrobial performance test of cotton-*g*-ZIF-8 are shown in Table 1. The synthesized cotton-*g*-ZIF-8 was tested with *Escherichia coli*, representing Gram-negative bacteria, *Staphylococcus aureus*, representing Gram-positive

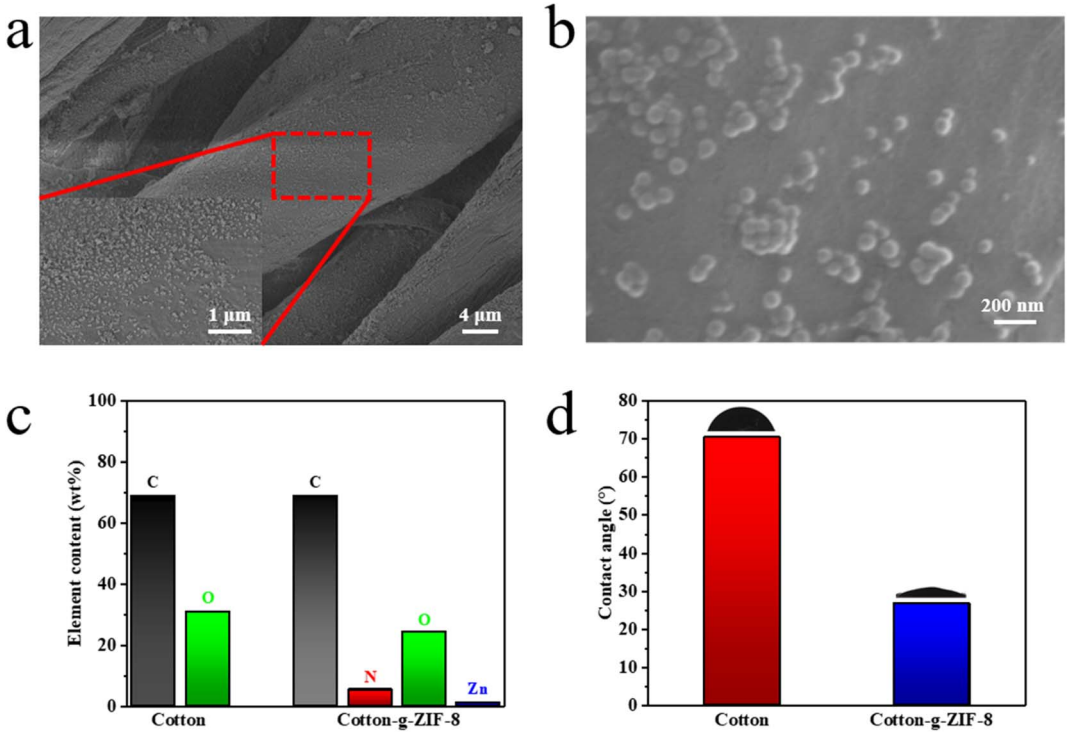

Fig. 4 (a) SEM image of cotton-*g*-ZIF-8. (b) SEM image of cotton-*g*-ZIF-8 (50 000×). (c) Element analysis of cotton and cotton-*g*-ZIF-8 (from XPS). (d) Water contact angle of cotton and cotton-*g*-ZIF-8.

Table 1 Antimicrobial performance test results of cotton-*g*-ZIF-8

Test organism (strain no.)	Concentration of inoculum (CFU mL^{-1})	The number of survived bacteria after wash-out at contact time (CFU)			Inhibition rate (%)
		—	Contact 0 h	Contact 24 h	
Escherichia coli 8099	1.4×10^5	Sample	—	<20	>99
		Control	2.6×10^4	5.2×10^7	
Staphylococcus aureus ATCC 6538	1.9×10^5	Sample	—	<20	>99
		Control	3.6×10^4	1.0×10^7	
Candida albicans ATCC 10231	1.3×10^5	Sample	—	5.6×10^2	>99
		Control	2.4×10^4	9.8×10^6	

bacteria, and *Candida albicans*, representing fungi, as antimicrobial test subjects. The test results surface that the synthetic cotton-*g*-ZIF-8 inhibits all three kind of microorganisms by more than 99%.

For the action of cotton-*g*-ZIF-8 on *Escherichia coli* can be seen form Fig. S5a–c.† At the moment of 0 h, *Escherichia coli* cells were added to the cotton. After 24 hours of incubation, the *Escherichia coli* on the control sample cotton fabric produced

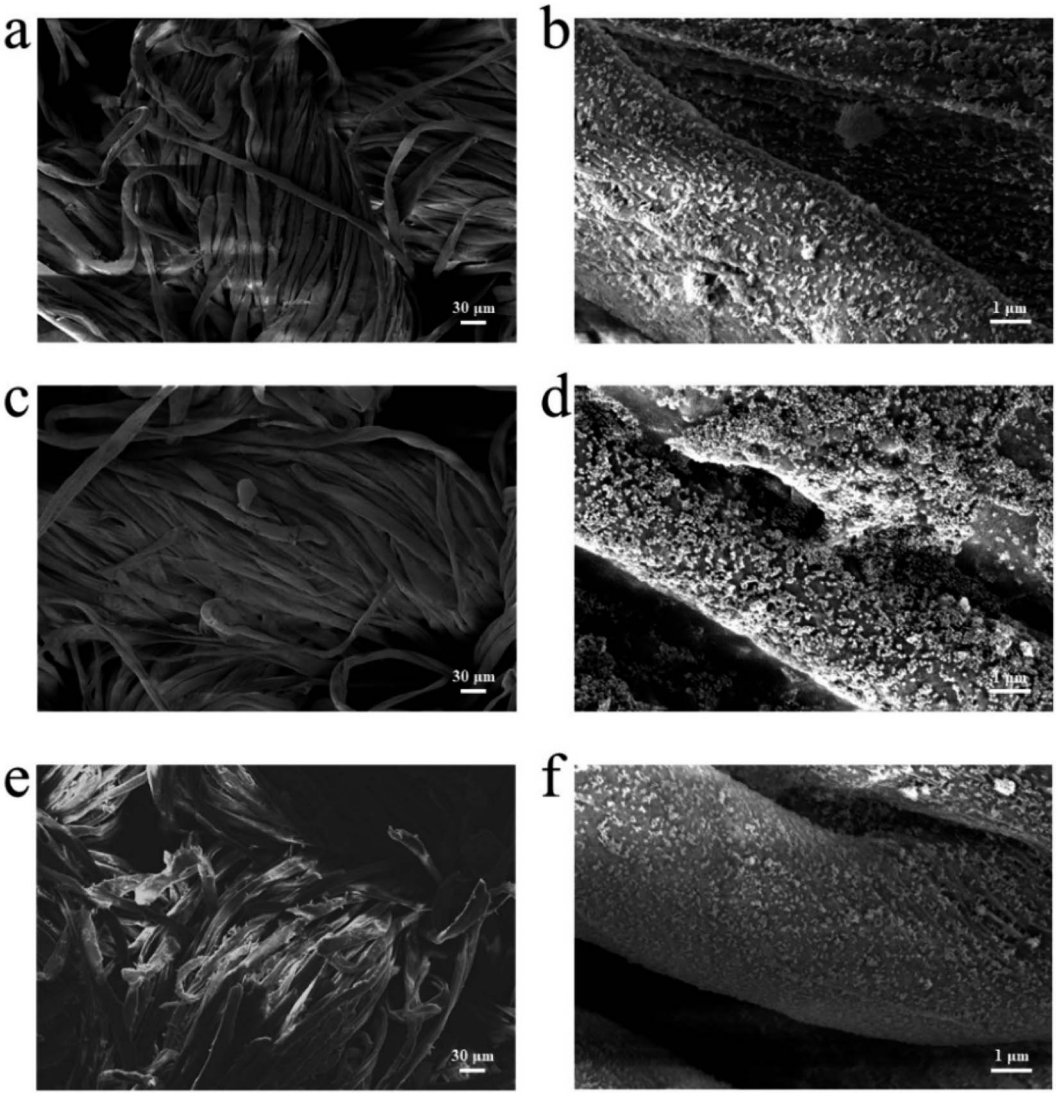

Fig. 5 Durability of cotton-*g*-ZIF-8. (a) 200× and (b) 10 000× SEM images of cotton-*g*-ZIF-8. (c) 200× and (d) 10 000× SEM images of cotton-*g*-ZIF-8 after 30 minutes dry cleaning. (e) 200× and (f) 10 000× SEM images of cotton-*g*-ZIF-8 after rubbed repeatedly for 2000 times.

a large number of cells by multiplication. In contrast, it was almost difficult to observe *Escherichia coli* on the cotton-*g*-ZIF-8. This shows that cotton-*g*-ZIF-8 can not only inhibit the growth of *Escherichia coli*, but also remove microorganisms by killing *Escherichia coli*. Similarly, the antibacterial performance of cotton-*g*-ZIF-8 against *Staphylococcus aureus* can be seen by Fig. S5d–f.† After 24 hours of multiplication, some colonies were visible on the control sample diluted 10 000 times, while almost no *Staphylococcus aureus* was observed on the undiluted cotton-*g*-ZIF-8. Fig. S5g–i† shows the antimicrobial performance of cotton-*g*-ZIF-8 against *Candida albicans*. After 24 hours of incubation, more colonies were visible on the 10 000-fold diluted from control sample, but only a few colonies were distributed on the undiluted cotton-*g*-ZIF-8 sample. This shows that cotton-*g*-ZIF-8 has a good antimicrobial effect on both bacteria and fungi. It can be concluded that this novel antimicrobial cotton fabric prepared by grafting ZIF-8 with electron beam radiation has excellent effect.

Benefit from the ZIF-8 particles grafted on the surface of cotton fibers, negatively charged bacteria and fungi can be adsorbed by electrostatic action.[49] On the one hand, the small nanostructure can be used to make it difficult for bacteria and fungi to adhere.[50] On the other hand, the slow degradation of ZIF-8 particles can release zinc ions with bactericidal effect, which can kill bacteria and fungi attached to the surface of cotton fibers.[51]

3.4. Durability of cotton-*g*-ZIF-8

Durability testing of cotton-*g*-ZIF-8 material provides information on the service life of this material. Here, dry cleaning and rub resistance of cotton-*g*-ZIF-8 were tested. Fig. 5a and b show the SEM images of cotton-*g*-ZIF-8 with 200× and 10 000× magnification, respectively. From the figures, it can be found that grafted ZIF-8 on cotton fiber has not changed in morphology. And ZIF-8 particles were attached to the cotton fibers more uniformly. Thus, this new cotton fabric possesses a modification at the microscopic level without changing its appearance, giving it the desired functionality. After a 30 minutes dry cleaning resistance test with tetrafluoroethylene dry cleaning agent, the appearance of the cotton fabric and the surface of the cotton fibers did not change significantly. This can be seen in Fig. 5c and d. ZIF-8 particles were still firmly fixed to cotton fibers. This indicates that the cotton-*g*-ZIF-8 can still maintain its expected properties after dry cleaning.

Fig. 5e and f show the SEM images of cotton-*g*-ZIF-8 fibers after 2000 times rubbing using the metal post tip. It can also be found that ZIF-8 is still held on the surface of the cotton fiber and has not changed significantly relative to the sample before rubbing. Although a few fibers on the surface of the cotton fabric were deformed or even broken after so many times of friction, its functional components ZIF-8 was still existed. It can be attributable to the strong covalent bonds between ZIF-8 and cotton fibers. Thus, the synthetic method of irradiation grafting makes this material have excellent durability.

4. Conclusions

In this paper, ZIF-8 was immobilized onto cotton fabric by covalent bonding using electron beam irradiation grafting method to prepare antimicrobial textiles with good durability. Characterization by FTIR, TGA, DSC, XRD, XPS and SEM proved that cotton-*g*-ZIF-8 was successfully synthesized. Antimicrobial performance test showed that cotton-*g*-ZIF-8 has excellent antimicrobial properties against *Escherichia coli*, *Staphylococcus aureus* and *Candida albicans*. The irradiation grafting method is simple and easy to perform with good reproducibility. By using irradiation grafting to attach the nanoparticles to cotton fabric through covalent bonding, the materials prepared have excellent durability. This research expands the development of energy-saving, environmentally friendly, and long-life functional textiles. It is promising to apply this technology to the preparation and mass production of a variety of functional textiles.

Conflicts of interest

There are no conflicts to declare.

Acknowledgements

This work was financially supported by the National Natural Science Foundation of China (Grant No. 11875313 and 12075153).

References

1 M. Jamal, W. Ahmad, S. Andleeb, F. Jalil, M. Imran, M. A. Nawaz, T. Hussain, M. Ali, M. Rafiq and M. A. Kamil, *J. Chin. Med. Assoc.*, 2018, **81**, 7–11.
2 C. R. Lee, I. H. Cho, B. C. Jeong and S. H. Lee, *Int. J. Environ. Res. Public Health*, 2013, **10**, 4274–4305.
3 A. P. Magiorakos, A. Srinivasan, R. B. Carey, Y. Carmeli, M. E. Falagas, C. G. Giske, S. Harbarth, J. F. Hindler, G. Kahlmeter, B. Olsson-Liljequist, D. L. Paterson, L. B. Rice, J. Stelling, M. J. Struelens, A. Vatopoulos, J. T. Weber and D. L. Monnet, *Clin. Microbiol. Infect.*, 2012, **18**, 268–281.
4 S. Siwal, Q. Zhang, A. Saini and V. K. Thakur, *J. Renewable Mater.*, 2020, **8**, 1543–1563.
5 S. Duan, R. Wu, Y.-H. Xiong, H.-M. Ren, C. Lei, Y.-Q. Zhao, X.-Y. Zhang and F.-J. Xu, *Prog. Mater. Sci.*, 2022, **125**, 100887.
6 M. Liang and X. Yan, *Acc. Chem. Res.*, 2019, **52**, 2190–2200.
7 Y. Huang, J. Ren and X. Qu, *Chem. Rev.*, 2019, **119**, 4357–4412.
8 Y. Tang, Y. Wu, W. Xu, L. Jiao, W. Gu, C. Zhu, D. Du and Y. Lin, *Adv. Agron.*, 2022, **1**, 12–21.
9 X. Zhang, X. Chen and Y. Zhao, *Nano-Micro Lett.*, 2022, **14**, 95.
10 L. Jiao, J. Y. R. Seow, W. S. Skinner, Z. U. Wang and H.-L. Jiang, *Mater. Today*, 2019, **27**, 43–68.
11 J. Canivet, A. Fateeva, Y. Guo, B. Coasne and D. Farrusseng, *Chem. Soc. Rev.*, 2014, **43**, 5594–5617.

12 R.-B. Lin, S. Xiang, W. Zhou and B. Chen, *Chem*, 2020, **6**, 337–363.
13 F. X. Llabrés i Xamena, A. Abad, A. Corma and H. Garcia, *J. Catal.*, 2007, **250**, 294–298.
14 J. Liu, D. Wu, N. Zhu, Y. Wu and G. Li, *Trends Food Sci. Technol.*, 2021, **109**, 413–434.
15 J. A. Lemire, J. J. Harrison and R. J. Turner, *Nat. Rev. Microbiol.*, 2013, **11**, 371–384.
16 J. Cao, X. Li and H. Tian, *Curr. Med. Chem.*, 2020, **27**, 5949–5969.
17 P. D. Ray, B. W. Huang and Y. Tsuji, *Cell. Signalling*, 2012, **24**, 981–990.
18 Q. Song, S. K. Nataraj, M. V. Roussenova, J. C. Tan, D. J. Hughes, W. Li, P. Bourgoin, M. A. Alam, A. K. Cheetham, S. A. Al-Muhtaseb and E. Sivaniah, *Energy Environ. Sci.*, 2012, **5**, 8359–8369.
19 A. Yuan, C. Hao, X. Wu, M. Sun, A. Qu, L. Xu, H. Kuang and C. Xu, *Adv. Mater.*, 2020, **32**, e1906580.
20 H. Kaur, G. C. Mohanta, V. Gupta, D. Kukkar and S. Tyagi, *J. Drug Delivery Sci. Technol.*, 2017, **41**, 106–112.
21 H. Chu, J. Shen, C. Wang and Y. Wei, *Colloids Surf., A*, 2021, **628**, 127388.
22 K. Wang, M. Qian, H. Qi, Q. Gao and C. Zhang, *Nanoscale*, 2020, **12**, 15663–15669.
23 M. Taheri, D. Ashok, T. Sen, T. G. Enge, N. K. Verma, A. Tricoli, A. Lowe, D. R. Nisbet and T. Tsuzuki, *Chem. Eng. J.*, 2021, **413**, 127511.
24 M. Taheri and T. Tsuzuki, *ACS Mater. Lett.*, 2021, **3**, 255–260.
25 P. Li, J. Li, X. Feng, J. Li, Y. Hao, J. Zhang, H. Wang, A. Yin, J. Zhou, X. Ma and B. Wang, *Nat. Commun.*, 2019, **10**, 2177.
26 L. Wang, C. Hu and L. Shao, *Int. J. Nanomed.*, 2017, **12**, 1227–1249.
27 E. A. Bryce, B. Velapatino, T. Donnelly-Pierce, H. A. Khorami, T. Wong, R. Dixon, E. Asselin, A. McGeer, J. A. Srigley and K. Katz, *Infect. Control Hosp. Epidemiol.*, 2022, **43**, 79–87.
28 L. Deschênes and T. Ells, *Adv. Colloid Interface Sci.*, 2020, **277**, 102106.
29 B. Gupta and N. Anjum, *J. Appl. Polym. Sci.*, 2001, **82**, 2629–2635.
30 N. Zhao, J. Peng, G. Liu, Y.-W. Zhang, W. Lei, Z. Yin, J. Li and Z. Maolin, *J. Mater. Chem. A*, 2018, **6**, 18458–18468.
31 H.-T. Wang, H.-Q. Jiang, R.-F. Shen, X.-J. Ding, C. Zhang, L.-F. Li and J.-Y. Li, *Nucl. Sci. Tech.*, 2018, **29**, 87.
32 S. Zhong, Y. Meng, Q. Ou and X. Shu, *J. Appl. Polym. Sci.*, 2005, **97**, 2112–2117.
33 L. Guo, B. Li and H. Wang, *J. Appl. Polym. Sci.*, 2011, **121**, 402–409.
34 B. Deng, R. Cai, Y. Yu, H. Jiang, C. Wang, J. Li, L. Li, M. Yu, J. Li, L. Xie, Q. Huang and C. Fan, *Adv. Mater.*, 2010, **22**, 5473–5477.
35 H. Li, X. Shen, H. Hua, J. Gao, Z. Wen, X. Wang, L. Peng, D. Wu, P. Zhang and J. Zhao, *Solid State Ionics*, 2020, **347**, 115246.
36 R. Ding, Y. Meng, Y. Qiao, M. Wu, H. Ma and B. Zhang, *Appl. Surf. Sci.*, 2022, **598**, 153665.
37 M. Yu, Z. Wang, H. Liu, S. Xie, J. Wu, H. Jiang, J. Zhang, L. Li and J. Li, *ACS Appl. Mater. Interfaces*, 2013, **5**, 3697–3703.
38 M. Yu, W. Li, Z. Wang, B. Zhang, H. Ma, L. Li and J. Li, *Sci. Rep.*, 2016, **6**, 22796.
39 W. Zou, Y. Chen, X. Zhang, J. Li, L. Sun, Z. Gui, B. Du and S. Chen, *Carbohydr. Polym.*, 2018, **202**, 246–257.
40 H. E. Clemmons, E. J. Clemmons and E. J. Brown, in *Electron Beam Pasteurization and Complementary Food Processing Technologies*, ed. S. D. Pillai and S. Shayanfar, Woodhead Publishing, 2015, pp. 11–25.
41 L. Woo and C. L. Sandford, *Radiat. Phys. Chem.*, 2002, **63**, 845–850.
42 Z. Jiang, Y. Wang, Y. Liu and X. Ren, *Fibers Polym.*, 2016, **17**, 1013–1017.
43 A. Alberti, S. Bertini, G. Gastaldi, N. Iannaccone, D. Macciantelli, G. Torri and E. Vismara, *Eur. Polym. J.*, 2005, **41**, 1787–1797.
44 J. Cravillon, R. Nayuk, S. Springer, A. Feldhoff, K. Huber and M. Wiebcke, *Chem. Mater.*, 2011, **23**, 2130–2141.
45 M. J. C. Ordoñez, K. J. Balkus, J. P. Ferraris and I. H. Musselman, *J. Membr. Sci.*, 2010, **361**, 28–37.
46 Y. Hu, H. Kazemian, S. Rohani, Y. Huang and Y. Song, *Chem. Commun.*, 2011, **47**, 12694–12696.
47 H. Yin, H. Kim, J. Choi and A. C. K. Yip, *Chem. Eng. J.*, 2015, **278**, 293–300.
48 J. H. Cavka, S. Jakobsen, U. Olsbye, N. Guillou, C. Lamberti, S. Bordiga and K. P. Lillerud, *J. Am. Chem. Soc.*, 2008, **130**, 13850–13851.
49 N. Ahmad, N. A. H. M. Nordin, J. Jaafar, A. F. Ismail and M. K. N. B. Ramli, *J. Environ. Chem. Eng.*, 2021, **9**, 105887.
50 F. Akbarzadeh, M. Motaghi, N. P. S. Chauhan and G. Sargazi, *Heliyon*, 2020, **6**, e03231.
51 R. Karimi Alavijeh, S. Beheshti, K. Akhbari and A. Morsali, *Polyhedron*, 2018, **156**, 257–278.